ORIGINAL ARTICLE

Groundwater flow evaluation using a groundwater budget model and updated aquifer structures at an alluvial fan of Echi-gawa, Japan

Heejun Yang[1,2]

Abstract

As groundwater is a vital water resource and plays an important role in sustainable use and environment maintenance, evaluating the groundwater flow is crucial. To quantitatively ascertain the groundwater flow at the Echi-gawa alluvial fan, Japan, groundwater budget was carried out by combining hydrogeological parameters (hydraulic gradient, hydraulic conductivity, and recharge rate) and modified aquifer structures (unconfined/confined aquifers and aquitards). The groundwater budget was calculated on the right bank (B–B′ cross section) and left bank (C–C′ cross section) of the Echi River, where the aquifer structures are significantly different. The total flow rate in the unconfined aquifer was 533.2×10^3 m^3/year, of which the outflow to the confined aquifer was 14% in B–B′, whereas the total flow rate in the unconfined aquifer was 433.7×10^3 m^3/year, of which the outflow to the confined aquifer was 2.7% in C–C′. The difference of the outflow to the confined aquifer between B–B′ and C–C′ is derived from the difference of the updated aquifer structures. The groundwater budget indicated that 5–20-holds amount of the groundwater infiltrates to more deeper aquifers than the aquitard the study targeted near the foot of mountains. The groundwater pumping in the confined aquifer in B–B′ affects the infiltration of the unconfined aquifer, which may control the groundwater quality. Results of the groundwater budget in this study are well corresponded to the previous studies. Although separating the groundwater pumping and the upward groundwater flow rate using the groundwater budget this study provided is unavailable due to lack of the hydraulic head in ATI in C–C′, the method used for this study is adequate to reproduce groundwater flow systems, which may be applicable to areas, where the aquifer structures are unestablished.

Keywords Alluvial fan · Flow rate · Groundwater flow · Groundwater budget · Pumping · Japan

Introduction

Groundwater is a vital water resource and plays an important role in sustainable use and environment maintenance because of its widespread availability and accessibility. In general, groundwater has a low-cost water source for public supply and domestic use, so groundwater has increasingly been exploited in preference to surface water (Zhou 2009; Takase and Fujihara 2019). Especially, groundwater of alluvial fans is the foremost water resource in arid/semiarid regions, because aquifers in alluvial fans include the abundance of groundwater (Hamada et al. 2008; Lu et al. 2020; Xiao et al. 2022). Alluvial fans are often distributed around the foot of mountains and show complicated geological structures by crustal deformation and composed of debris-flow deposits transported from mountainous areas (Sakata et al. 2016). Farmlands and livestock, therefore, are usually substituted for the alluvial fans located in the foot of mountains due to the high permeability of the deposits (Yamanaka and Sakamoto 2016). Consequently, the groundwater depletion and deterioration of water quality in alluvial fans have been concerned due to anthropogenic interferences, such as nitrogen loads and groundwater abstracts (Shimada et al. 2015; Yin et al. 2019; Lu et al. 2020; Cervi and Tazioli 2021).

To prevent reducing groundwater resources and deterioration of groundwater quality, numerous studies subjecting to groundwater flow systems have been conducted using analytical and numerical approaches (e.g., Tóth and Millar 1983; England and Freeze 1988). The hydraulic gradient

✉ Heejun Yang
heejun@sci.u-toyama.ac.jp

1 Institute for Geothermal Sciences, Graduate School of Science, Kyoto University, 3088-176 Noguchibaru, Beppu, Oita 874-0903, Japan

2 Graduate School of Science and Engineering, University of Toyama, 3190 Gofuku, Toyama 930-8555, Japan

has both a magnitude and direction of groundwater flow, and its velocity is proportional to the magnitude of the hydraulic gradient and the hydraulic conductivity of an aquifer (Barackman and Brusseau 2002). These parameters explain, where the groundwater flows and how long the groundwater takes to pass through a target region. Changes in the hydraulic gradient and groundwater levels are derived from changes in precipitation pattern and land use (i.e., recharge), and overexploitation, which could cause progressive depletion of the groundwater resource (Viaroli et al. 2018). Identification of aquifer structures (e.g., unconfined/confined aquifers and aquitards) is a crucial task to quantitatively evaluate the available groundwater resource, because the flow rate is mainly dependent on the hydraulic conductivity and depth of aquifers (Tóth and Hayashi 2010; Demiroglu 2019).

Groundwater budget is the most effective method to quantify the groundwater resource, which calculates all inputs, outputs, and changes in an aquifer (Yamamoto 1983; Demiroglu 2019). The groundwater balance assumes that the inputs and outputs of an aquifer are equal over a given time interval, considering any change in storage. The groundwater budget has usually been used for understanding safe yield (Alley and Leake 2004; Zhou 2009; Viaroli et al. 2018), surface–subsurface interaction (Ibrakhimov et al. 2018; Alattar et al. 2020), and groundwater flow system (He et al. 2008; Gu et al. 2017; Viaroli et al. 2018). For instance, Gu et al. (2017) reported that the discharge rate of the shallow flow system was four times higher than that of the middle flow system using the numerical model in the Qaidam basin, China. Viaroli et al. (2018) revealed a severe water deficit of approximately 40% of the total groundwater outflow in the Riardo Plain aquifer by combining the groundwater budget calculation with long-term (more than 20 years) aquifer monitoring. They also mentioned that the groundwater budget could not be calculated without the complete knowledge of the boundary condition of a hydrogeological basin. Genereux et al. (2005) stated that one of the most difficult watershed fluxes to quantify is interbasin groundwater flow (i.e., deep groundwater flow that passes beneath watershed topographic boundaries). In other words, knowing aquifer structures is important in calculating the groundwater budget.

The Echi-gawa alluvial fan, Japan utilizes groundwater as a water resource for residents. This artificial groundwater use caused the depression of the groundwater levels and reduced vital groundwater resources in this region (Kobayashi et al. 2008). Many studies were conducted for understanding groundwater flow systems using chemical compositions (Kobayashi et al. 2010), groundwater temperatures (Yang et al. 2011), hydrogeological property (Oishi et al. 2008), and a numerical simulation (Hijii et al. 2008). However, the studies were investigated without accurate aquifer

divisions in the study area, because the evaluation of geologic columns was not supported sufficiently.

The wells for irrigation and water supply are distributed in the Echi-gawa alluvial fan, but few studies have been carried out to understand the geologic structure using observation wells. Lithologic logs of the wells are described based on pieces of slime obtained by non-core drilling, which is not reliable in assessing geological structures. However, the data of the wells usually accompany the electric logs, which is an efficient method to understand aquifer structures (Japanese Geotechnical Society 2005). Yang and Mitamura (2012) established the modified aquifer structures using the electric logs of the wells with gravity anomalies and standard stratigraphy in the study area. However, the accurate groundwater flow systems are still unclear. The present study was conducted to quantitatively ascertain the groundwater flow using the groundwater budget by combining hydrogeological parameters (hydraulic gradient, hydraulic conductivity, and recharge rate) and modified aquifer structure (unconfined/confined aquifers and aquitards) at the Echi-gawa alluvial fan, Japan. The groundwater budget was calculated in two cross sections, where the aquifer structures are significantly different.

Study area

Echi-gawa alluvial fan is located in the western foot of the Suzuka Mountains, Japan, which is bounded by the Yokaichi Hill, Hyakusaiji, Kozubada, and Eigenji faults (Fig. 1). Geology in this area consists of the Paleo-Mesozoic basement rocks, the Plio-Pleistocene Kobiwako Group, Pleistocene terrace deposits, and Holocene alluvial deposits in ascending order. The basement rocks distributed in the eastern mountain areas are composed of Paleo-Mesozoic sedimentary rocks and Cretaceous volcanic rocks named Koto Rhyolite (Oishi et al. 2008). The periphery of the Echi river is composed of the Pleistocene terrace deposits, which are divided by the three terrace deposits, and Holocene alluvial deposits (Ikeda et al. 1979; Yokoyama et al. 1979; Harayama et al. 1989). Hydraulic conductivity obtained by pumping and slug tests ranged from 10^{-3} to 10^{-4} m/s at the terrace and alluvial deposits, from 10^{-4} to 10^{-6} m/s at the sand and gravel layers in the Kobiwako Group, and $< 10^{-7}$ m/s at the slit and clay layers in the Kobiwako Group (Oishi et al. 2008).

Methods

To assign a groundwater budget method, hydrogeology parameters such as hydraulic conductivity, hydraulic gradient, recharge rate from the surface, and aquifer thickness are collected. Methods to obtain these parameters are shown
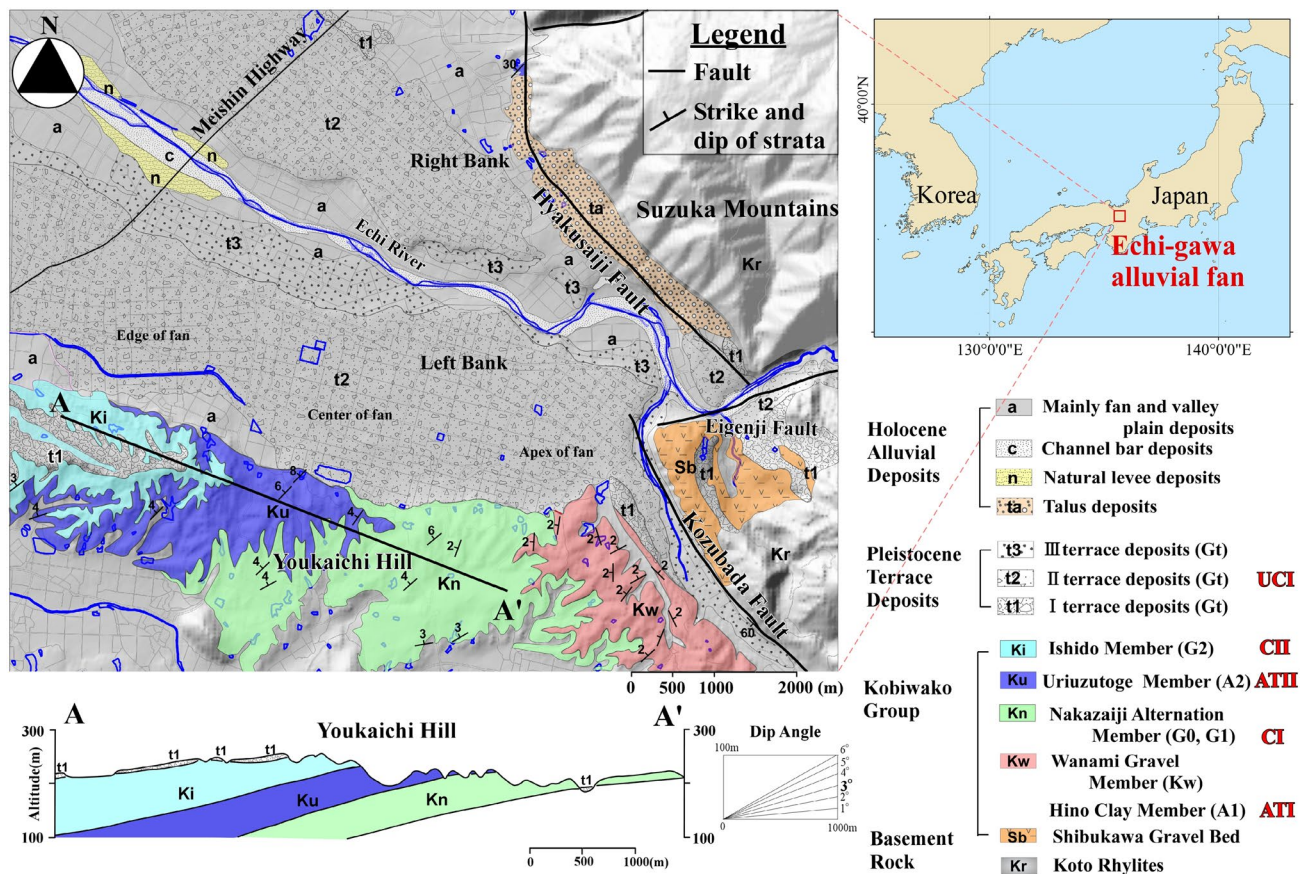
Fig. 1 Study area and the geology map in Echi-gawa alluvial fan, Japan (referring to Harayama et al. 1989). Red characters express the aquifer units

in Fig. 2; step 1 explains how the aquifer divisions were performed, and step 2 expresses what methods were used to obtain the hydraulic gradient and the hydraulic conductivity of the unconfined and confined aquifers on cross sections that were chosen at most dominant groundwater flow paths, finally step 3 shows a method for the groundwater budget. The step 1 and step 2 methods are briefly reviewed; then the groundwater budget is precisely explained below.

## Aquifer structure and thickness

Geologic columns with electric logs at 44 wells in the study area were revised based on the specific resistivity (Yang and Mitamura 2012) (Figs. 3 and S1). The original description of sandy-, silty-, and gravelly- in the geologic column was revised to 5 lithologic divisions of terrace gravel, gravel, sand, sandy silt, and mud. For example, around the depth of 100 m at the R19 site, the original column (OG) shows the alternation of sand and mud (Fig. 3a). Because the specific resistivity (SR) of sand layers in this part is high (50–60 Ωm), these sand layers were modified to gravel layers in the revised column (Re). At the L26 site, sedimentary

layers are roughly divided into several parts in the original column. The specific resistivity of this site well fluctuates, indicating the lithologic alternation. The description in the original column was modified to the alternation of mud, sand, and gravel.

The revised geologic columns are compared to the gravity anomaly (Nishimura 1979). The gravity anomaly in this area ranges from − 30 to – 43 mgal (Fig. 3b). The trend of the gravity anomaly gradually decreases from the mountain foot to westward. In the right bank of the Echi-gawa River, the relatively intensive transition zone is distributed along the edge of the fan. This gravity anomaly intensive zone suggests a strong flexure of the Kobiwako Group in this area (Yang and Mitamura 2012), which was entrapped in the revised aquifer structure showing the steep dip angle of the aquifer units.

Quaternary sediments, based on the revised columns and the gravity anomaly, are divided into seven units of A1, Kw, G0, G1, A2, G2, and Gt in ascending order, which are corresponded with the Hino Clay, Wanami Gravel, Nakazaiji Alternation, Uriuzutoge and Ishido Members in the Kobiwako Group, and terrace deposits, respectively (Table 1 and
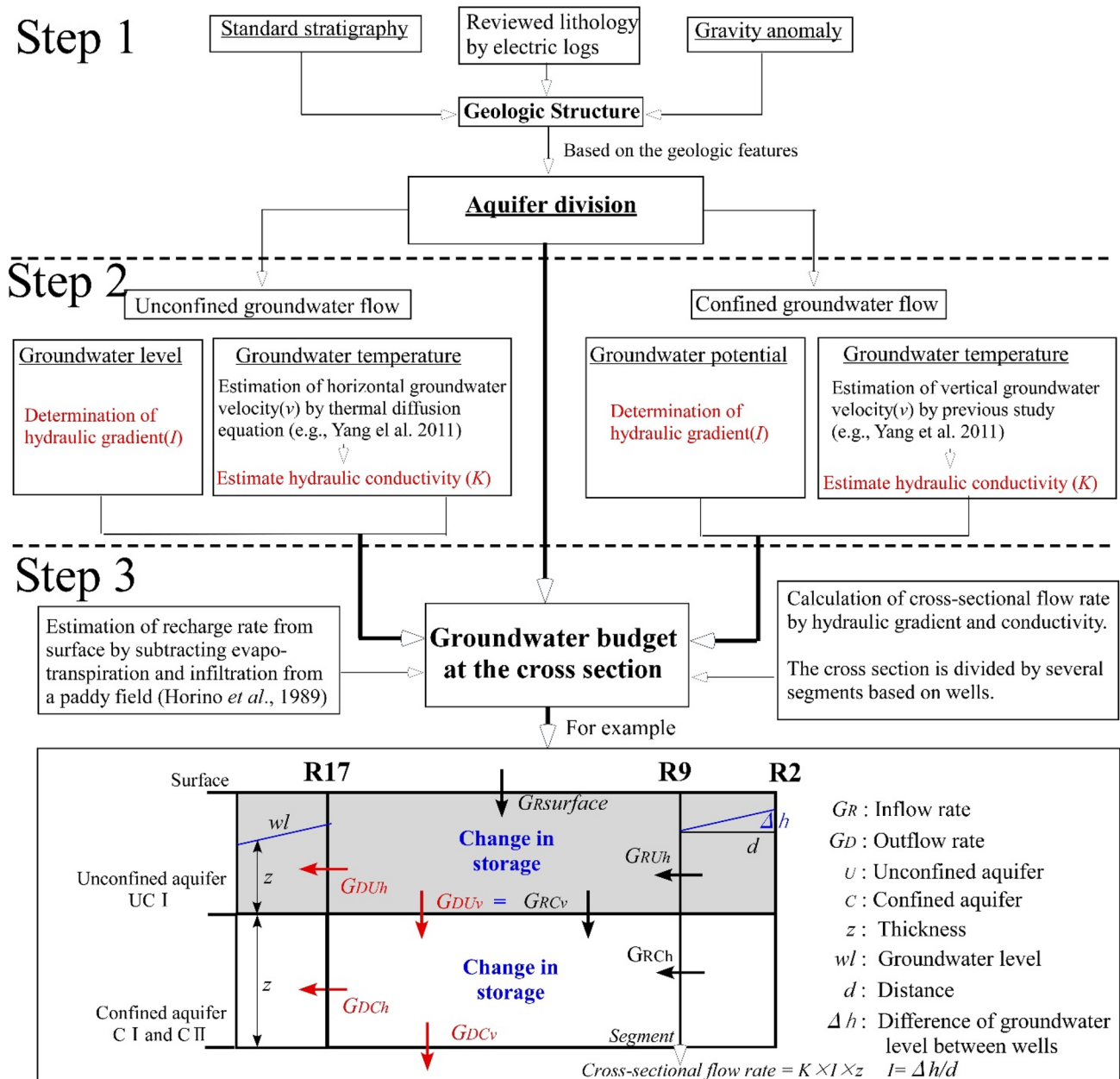
Fig. 2 Flow chart to evaluate the groundwater budget at the cross section. R2, R9, and R17 are wells. Subscripts h and v indicate the horizontal and vertical flows, respectively. K is the hydraulic conductivity. I stands for the hydraulic gradient

Fig. 1). These lithostratigraphic units in this area are divided into five aquifer units of ATI, CI, ATII, CII, and UCI (ATII and ATI are aquitards, and CI and CII are confined aquifers, and UCI is unconfined aquifer) in ascending order. Seven cross-sectional maps were produced by Yang and Mitamura (2012) (Fig. S2). Particularly, the *B–B′* and *C–C′* cross sections correspond to dominant groundwater flow paths (Kobayashi et al. 2011). The groundwater budget was calculated on the right bank (*B–B′*) and left bank (*C–C′*) of the Echi River, where the aquifer structures are significantly different (Fig. 4b).

Hydraulic gradient and conductivity

The hydraulic gradient was estimated by groundwater level contour in the unconfined aquifer in 2007 (Hamada et al. 2008; Fig. 4a) and groundwater potential in the confined aquifer in annual mean groundwater head in 2007 (Kobayashi et al. 2010; Fig. 4c). The groundwater levels and heads at the observation wells were indicated in Tables 2 and 3 with the distance of each well. Darcy velocity of the groundwater was calculated by groundwater temperature using analytical expressions in the unconfined and confined
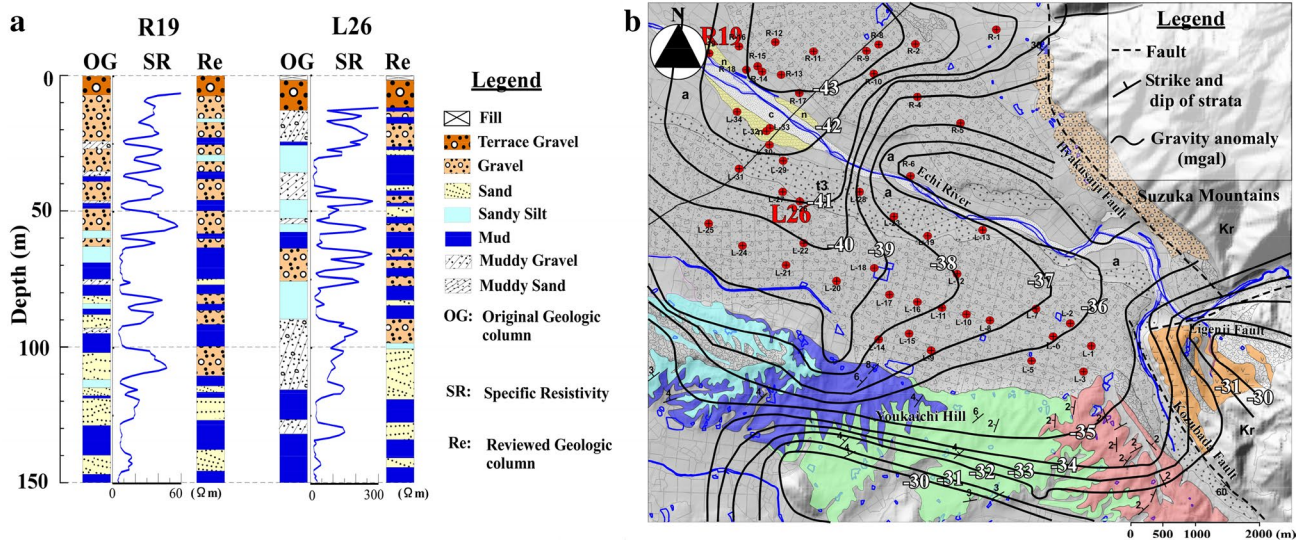
Fig. 3 Examples of **a** the original geologic column (OG), revised geologic column (Re), and specific resistivity (SR), and **b** distribution of the gravity anomaly in the study area referring to Nishimura (1979). Red circles represent the wells accompanied with electric logs

Table 1 Geological correlation between Quaternary sediments on the Echi-gawa alluvial fan and the standard stratigraphy of the Youkaichi Hill

| Geologic age	Standard stratigraphy on Youkaichi Hill			Lithology of the Echi-gawa alluvial fan	
	Formation	Member		Lithologic Unit (Aquifer Unit)	Lithology
Middle/Late Pleistocene	Terrace Deposits	Terrace III, II, I		Gt (UCI)	Mainly consist of terrace gravel and intercalate sand and rare mud
Early Pleistocene	Kusatsu Formation	Ishido Member		G2 (CII)	Gravelly layers with alternation of sand and mud
		Uriuzutoge Member		A2 (ATII)	Alternation layers with gravel, sand and mud
	Kamo Formation	Nakazaiji Alternation Member	Wanami Gravel Member	G1, G0 (CI) Kw	Gravelly layers with alternation of gravel, sand and mud
		Hino Clay Member		A1 (ATI)	Mud layers with alternation of mud and sand

aquifers (e.g., Yang et al. 2011). The Darcy velocity of the unconfined aquifer was calculated using the horizontal one-dimensional heat advection–diffusion equation. This study shows the solution of it as below:

$$ax = -\ln(\Delta T_x/\Delta T_0) \tag{1}$$

$$a = \left[\left(U^2 + V^4/4\right)^{\frac{1}{2}} + V^2/2\right]^{\frac{1}{2}} - V \tag{2}$$

$$U = \pi c\rho/k\tau, V = v_x c_o \rho_0/2k \tag{3}$$

where k stands for the thermal conductivity (cal/cm s°C), $c\rho$ and $c_o\rho_0$ are the heat capacity (cal/cm°C) of sediment and water, respectively, ΔT_x is the groundwater temperature change width at distance x (°C), ΔT_0 is the groundwater temperature change width at distance $x = 0$ (°C), v_x represents the horizontal Darcy velocity (m/s), τ is the period (s), U, V, a are the constant. As the unconfined aquifer consists of sand and gravel layers, k and $c\rho$ were set to be 4.5×10^{-3} cal/cm s°C and 0.6 cal/cm°C, respectively. $c_o\rho_0$ was the 1.0 cal/cm°C (Yang et al. 2011). The observed groundwater temperature in the unconfined aquifer was used to the ΔT_0 and ΔT_x. The velocity was estimated by fitting the type curves of v_x vs. ΔT_0 (Fig. S3). The estimated velocity was 4.0×10^{-3} m/s on the right bank of Echi River (B–B′) and 3.0×10^{-3} m/s
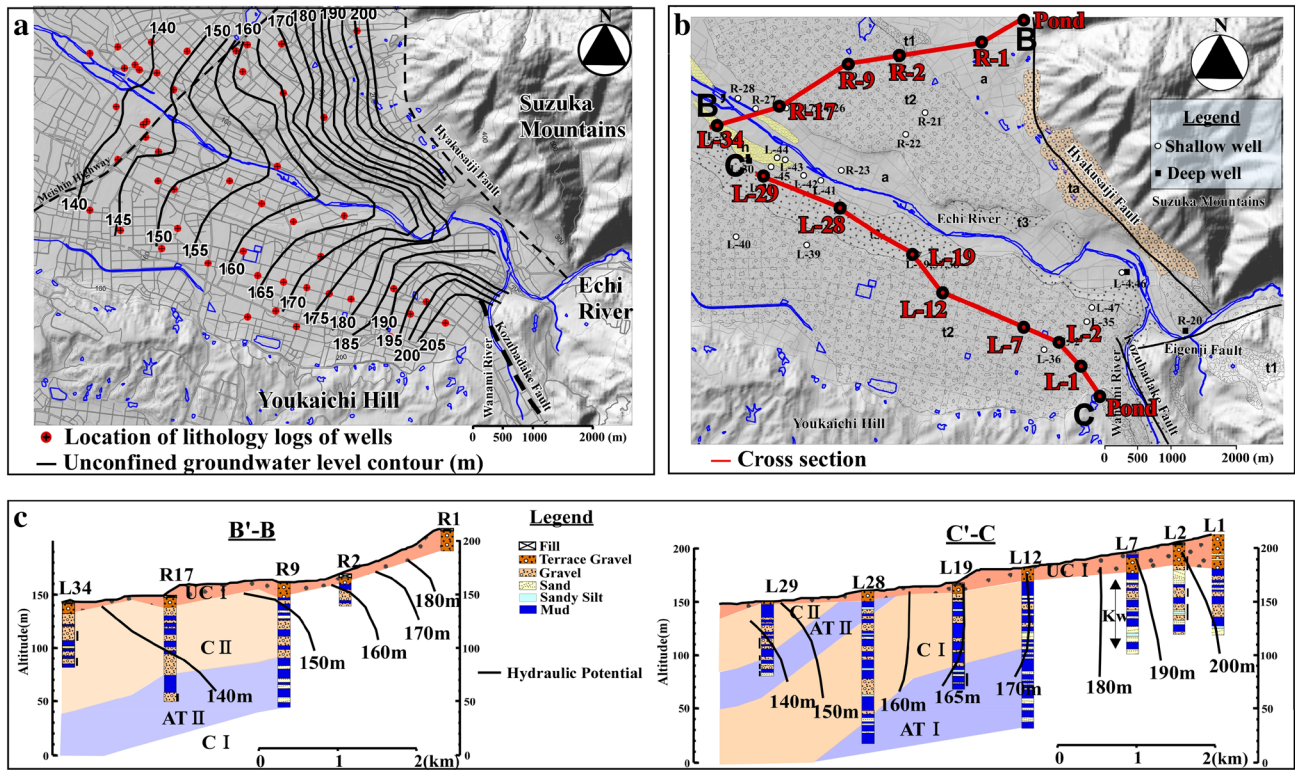
Fig. 4 **a** Unconfined groundwater level contour, **b** location of *B–B′* and *C–C′* cross sections with wells, and **c** the hydraulic potential lines of the confined aquifers in *B–B* and *C–C′*

Table 2 Calculated groundwater velocity and flow rate on the right bank river (*B–B′*)

UCI	$K = 4.0 \times 10^{-3}$ m/s					
	Pond	R1	R2	R9	R17	L34
d (m)		600	1258	516	1485	899
I		0.05	0.029	0.017	0.01	0.009
wl (m)	235	205	168	159	145	137
AB (m)		191	158	147	139	133
z (m)		14	10	12	6	4
v (m/s)		2.0×10^{-4}	1.2×10^{-4}	7.0×10^{-5}	3.8×10^{-4}	3.6×10^{-4}
v_r (m/s)		6.7×10^{-4}	3.9×10^{-4}	2.3×10^{-4}	1.3×10^{-4}	1.2×10^{-4}
$n = 0.3$						
Q (m³/year)		294.3×10^3	123.6×10^3	87.8×10^3	23.7×10^3	14.9×10^3
CII	$K = 7.4 \times 10^{-5}$ m/s					
	Pond	R1	R2	R9	R17	L34
I				5.8×10^{-3}	3.3×10^{-3}	8.9×10^{-3}
z (m)				55	65	80
v_r (m/s)				4.3×10^{-6}	2.4×10^{-6}	6.6×10^{-6}
$n = 0.1$						
Q (m³/year)				7.4×10^3	5.0×10^3	16.6×10^3

d is the distance, *I* is the hydraulic gradient, wl is the groundwater level, AB is the aquifer boundary, *z* is the aquifer thickness, *v* is the groundwater velocity, v_r is the fluid velocity (actual groundwater velocity), *n* is the porosity, *K* is the hydraulic conductivity, and *Q* is the flow rate

Table 3 Calculated groundwater velocity and flow rate on the left bank river (C–C′)

UCI	$K = 3.0 \times 10^{-3}$ m/s							
	Pond	L1	L2	L7	L12	L19	L28	L29
d (m)		482	481	600	1321	807	1219	1266
I		0.025	0.027	0.017	0.013	0.007	0.008	0.008
wl (m)	222	210	197	187	170	164	154	144
AB (m)		181	184	177	168	158	150.5	141
z (m)		29	13	10	2	6	3.5	3
v (m/s)		1.0×10^{-4}	1.1×10^{-4}	6.7×10^{-5}	5.2×10^{-5}	3.0×10^{-5}	3.3×10^{-5}	3.2×10^{-5}
v_r (m/s)		3.3×10^{-4}	3.6×10^{-4}	2.2×10^{-4}	1.7×10^{-4}	9.9×10^{-5}	1.0×10^{-4}	1.0×10^{-4}
$n = 0.3$								
Q (m³/year)		230.1×10^3	107.3×10^3	52.7×10^3	16.3×10^3	14.0×10^3	9.0×10^3	7.4×10^3
CI	$K = 7.4 \times 10^{-5}$ m/s							
	Pond	L1	L2	L7	L12	L19	L28	
I					0.012	0.0062	0.0074	
z (m)					70	80	95	
v_r (m/s)					8.9×10^{-6}	4.6×10^{-6}	5.5×10^{-6}	
$n = 0.1$								
Q (m³/year)					19.6×10^3	11.6×10^3	16.4×10^3	

The parameters are the same as Table 2

on the left bank of Echi River (C–C′), which was applied to the UCI aquifer.

The horizontal Darcy velocity of the confined aquifer was given as (Sakura 1984):

$$\frac{T_m}{T_1} = \frac{1}{2} + \frac{T_2}{2T_1} + \frac{2}{\pi^2} \sum_{n=1}^{\infty} \frac{1}{n^2}\left(\frac{T_1}{T_2}\cos n\pi - 1\right)\exp(-pn^2\pi^2)(1 - \cos n\pi) \tag{4}$$

$$p = kx/v_x c_o \rho_0 L^2 \tag{5}$$

where T_m signifies the mean temperature (°C), T_1 and T_2 are the temperature of the lower and upper boundaries of the confined aquifer (°C), p is the constant, L stands for the aquifer thickness (m), and x expresses the length of the aquifer (m). The parameters used were $x = 4000$ m, $L = 70$ m, $k = 4.3 \times 10^{-3}$ cal/cm s°C, $T_m = 16.5$ °C, $T_1 = 16.8$ °C, and $T_2 = 16.3$ °C. The estimated velocity was 7.4×10^{-5} m/s (Yang et al. 2011), which was applied to the CI and CII aquifers.

For the groundwater budget, hydraulic conductivity was calculated from the estimated velocity of the unconfined and confined aquifers using

$$K = v_x/I \tag{6}$$

where K stands for the hydraulic conductivity (m/s), v_x denotes the Darcy velocity (m/s), and I signifies the hydraulic gradient (dimensionless).

Groundwater budget

Change in groundwater storage in aquifers is expressed as (Yamamoto 1983)

$$\Delta S = G_r - G_d \tag{7}$$

where G_r is recharge or inflow rate in an arbitrary aquifer, and G_d is the discharge or outflow rate in an arbitrary aquifer. The change in groundwater storage (ΔS) balances with inflow (G_r) and outflow (G_d) rate and can be considered as the steady state when the inflow and outflow rates are equilibrium (Yamamoto 1983; Viaroli et al. 2018). Assuming that the groundwater storage does not change in an isotropic/homogeneous aquifer and contours of the groundwater levels are parallel distributions, the inflow and outflow rates can be inferred by the cross-sectional area. In other words, if the groundwater has a dominant flow path, the inflow and outflow rates in the cross-sectional area would be equivalent.

The cross sections of B–B′ and C–C′ were divided by 4 and 6 segments based on the well locations, respectively. The cross-sectional inflow and outflow rates were calculated at the wells using fluid velocity (or actual groundwater

velocity) and the aquifer thickness on the unconfined and confined aquifers separately (Earle 2019; step 3 in Fig. 2). The fluid velocity in a well was calculated by the hydraulic conductivity (K), hydraulic gradient (I) between two wells, and porosity:

$$v_r = \frac{KI}{n}. \tag{8}$$

Therein, v_r represents the fluid velocity (m/s) and n expresses the porosity.

For instance, the change in storage of the unconfined (ΔS_U) and confined aquifer (ΔS_C) between well R9 an R17 (i.e., a segment) was calculated:

$$\Delta S_U = G_{R_{surface}} + G_{RUh} - G_{DUh} - G_{DUv} \tag{9}$$

$$\Delta S_C = G_{RCv}(= G_{DUv}) + G_{RCh} - G_{DCh} - G_{DCv} \tag{10}$$

$$G_{RUh} = v_r \times z \tag{11}$$

where G_{RUh} signifies the inflow rate across the wells in the unconfined aquifer (m³/year), G_{DUh} denotes the outflow rate across the wells in the unconfined aquifer (m³/year), G_{DUv} represents the vertical outflow rate to the confined aquifer (m³/year), G_{RCv} stands for the vertical inflow rate from the unconfined aquifer (m³/year), G_{RCh} expresses the inflow rate across the wells in the confined aquifer (m³/year), G_{DCh} represents the outflow rate across the wells in the confined aquifer (m³/year), G_{DCv} is the outflow rate from the confined aquifer to a deep aquifer (m³/year), and z indicates the thickness between the groundwater level and the bottom of the unconfined aquifer, or the aquifer thickness in the confined aquifer (m). Since the cross sections correspond to dominant groundwater flow paths, a right-angled groundwater flow can be negligible. Thus, it was set to 1 m for the flow rate calculation. The porosities were set to 0.3 in the unconfined aquifer and 0.1 in the confined aquifer to obtain the fluid velocity (v_r), because the terrace gravel is dominant in the unconfined aquifer and the gravel, sand, and mud are dominant in the confined aquifer. The annual analysis of the groundwater budget was selected, because it covers a hydrological year (i.e., the groundwater level rises and falls for a year) which is suitable to evaluate the groundwater flow system.

Inflow rate from the surface to the unconfined aquifer ($G_{R_{surface}}$) was estimated by rainfall recharge and infiltration rate from paddy fields, because the paddy fields are widely distributed in the cross sections of B–B' and C–C'. The infiltration rate from the paddy fields was 740 mm/year referring to Horino et al. (1989). The rainfall recharge was 170 mm/year if the surface discharge was 30% of annual rainfall. The rainfall recharge was estimated by subtracting evapotranspiration calculated by the Thornthwaite method (722 mm/year; Thornthwaite 1948) and surface discharge (380 mm/year),

from annual rainfall in 2007 (1272 mm/year). Consequently, the inflow rate from the surface to the unconfined aquifer was 0.91 m/year. For instance, the inflow rate from the surface between well R9 and R17 was calculated by

$$G_{R_{surface}} \times d \tag{12}$$

where d is the distance between the wells (1485 m × 0.91 m/year × 1 m = 1.4 × 10³ m³/year; Fig. 5). However, 30% annual rainfall as the surface discharge has the uncertainty, because it was not derived from previous studies in the area, thus the present study treated the surface discharge as a variable. Therefore, 10%, 20%, 30%, and 40% annual rainfalls were applied to calculate the rainfall recharge. The influence of these variables was compared to the horizontal groundwater flow rate against the storage.

Results

Cross-sectional flow rate at the wells

The cross-sectional flow rate in B–B' and C–C' was calculated using Eq. (8), the distance between the wells, the elevation, the groundwater level and head, the porosity, and the aquifer thickness. The results are represented in Table 2 for B–B' and Table 3 for C–C'.

In B–B', the cross-sectional flow rates were calculated at five wells. The flow rates at well R1 and well L34 in the unconfined aquifer (UCI) were 294.3 × 10³ m³/year and 14.9 × 10³ m³/year, respectively. The flow rate decreased as the groundwater flows from the mountain area to the Echi River. The flow rates in the confined aquifer (CII) ranged from 5.0 × 10³ m³/year at well R17 and 16.6 × 10³ m³/year at well L34, which are relatively lower flow rates than those of the unconfined aquifer. In C–C', the cross-sectional flow rates were calculated at seven wells. The flow rates at well L1 and well L29 in the unconfined aquifer (UCI) were 230.5 × 10³ m³/year and 10.1 × 10³ m³/year, respectively. The flow rate decreased the same as B–B'. The flow rates in the confined aquifer (CI) ranged from 11.6 × 10³ m³/year at well L19 and 19.6 × 10³ m³/year at well L12. The cross-sectional flow rates in UCI and CI were the same magnitude at wells L12. L19, and L28.

Rainfall recharge

Since the surface discharge has the uncertainty, the 10%, 20%, 30%, and 40% of annual rainfalls were applied to calculate the rainfall recharge, and the influence of these variables was compared. Equation (12) was used for the calculation at four segments (S1, S2, S3, and S4) in B–B' and at six segments (S1, S2, S3, S4, S5, and S6) in C–C'.

Fig. 5 Groundwater budget in **a** *B–B′* and **b** *C–C′*. Blue numbers are the changes in storage in each segment. * indicates the estimated pumping rate in this study. S stands for the segment. UCI is unconfined aquifer; CI and CII are confined aquifers; ATI and ATII are aquitards
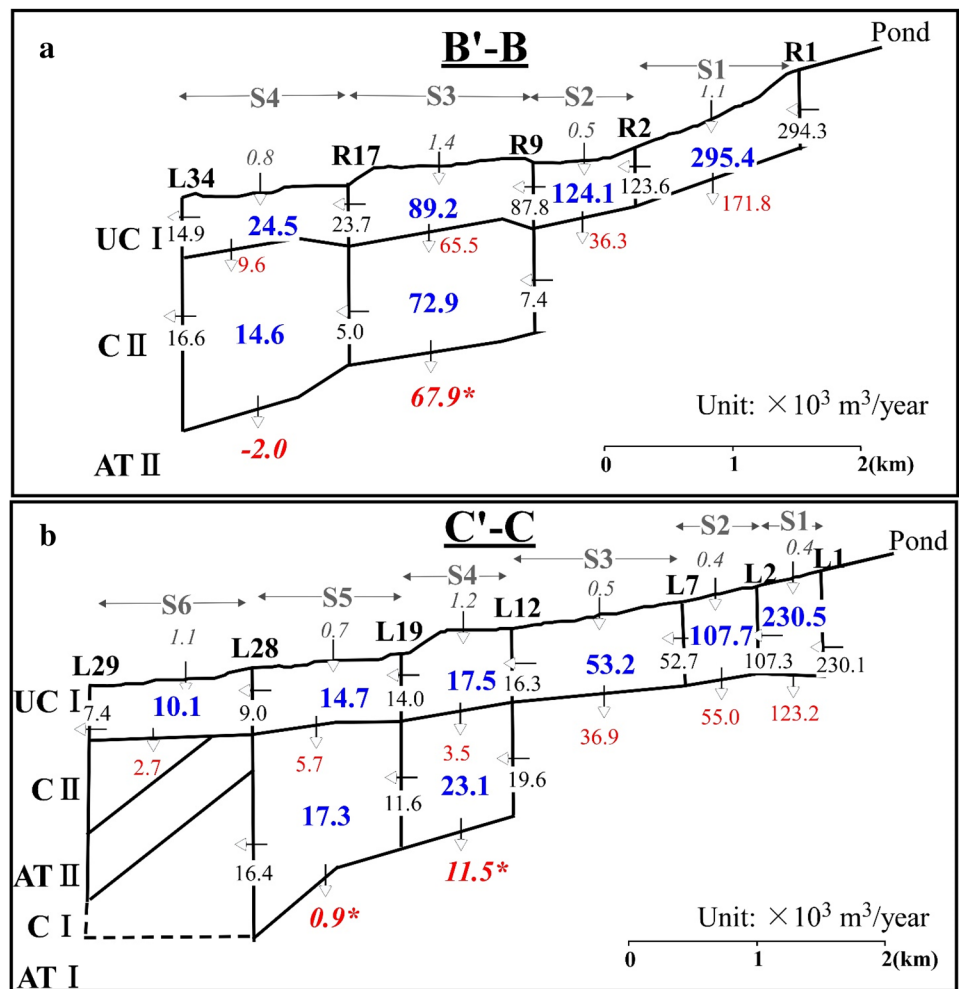
The segment means the distance between the wells (e.g., S1 in *B–B′* is the distance between well R1 and well R2). The influence was calculated from the inflow rate from the surface to the unconfined aquifer divided by the storage at each segment, which was expressed as a percentage. The results are expressed in Table 4. The rainfall recharge increases as the groundwater flows (from S1 to S4 and S6) in *B–B′* and *C–C′*. The average ± standard deviation of the

Table 4 Influence that was calculated from the inflow rate from the surface to the unconfined aquifer divided by the storage at each segment

Influence against storage in *B–B′* (%)					
Rainfall recharge	S1	S2	S3	S4	
40%	0.3	0.3	1.3	2.9	
30%	0.4	0.4	1.5	3.3	
20%	0.4	0.4	1.7	3.8	
10%	0.5	0.5	1.9	4.2	
Influence against storage in *C–C′* (%)					
Rainfall recharge	S1	S2	S3	S4	S5	S6
40%	0.2	0.3	0.9	6.0	4.3	9.5
30%	0.2	0.4	1.0	6.9	5.0	10.9
20%	0.2	0.5	1.2	7.8	5.6	12.2
10%	0.2	0.5	1.3	8.6	6.3	13.5

influence of the 10%, 20%, 30%, and 40% of annual rainfalls were $0.4 \pm 0.1\%$ at S1, $0.4 \pm 0.1\%$ at S2, $1.6 \pm 0.3\%$ at S3, and $3.6 \pm 0.6\%$ at S4 in B–B'. In C–C', those were $0.2 \pm 0.0\%$ at S1, $0.4 \pm 0.1\%$ at S2, $1.1 \pm 0.2\%$ at S3, $7.3 \pm 1.1\%$ at S4, $5.3 \pm 0.8\%$ at S5, and $11.6 \pm 1.7\%$ at S6. This means that the influence of the changes in surface discharge is at most 3.4% against the storage in the study year and area. Therefore, the groundwater budget was calculated using the 30% of annual rainfall because of the less influence of the variables.

Groundwater budget

In B–B', the groundwater budget in four segments is shown in Fig. 5a. The vertical outflow rates from UCI to CII in the segments 1 and 2 (S1 and S2 in Fig. 5a) were 171.8×10^3 m³/year and 36.3×10^3 m³/year, and the inflow rate at S3 in CII was 7.4×10^3 m³/year. This indicates that 5–20-holds amount of the groundwater infiltrates to deeper aquifers than CII near the foot of mountains. The vertical outflow rate from UCI to CII at S3 was 65.5×10^3 m³/year. In contrast, the inflow and outflow rates at S3 in CII were 7.4×10^3 m³/year and 5.0×10^3 m³/year, respectively. It reflects that a 67.9×10^3 m³/year amount is vertically discharged to ATII. However, it is unlikely that this vertical flow happens, because ATII is an aquitard. According to Sawada et al. (2008), the sustained groundwater pumping for residents is taking place near the S3 area. Therefore, it is reasonable to consider the vertical flow rate to ATII as the pumping rate. At S4 in CII, the inflow and outflow rates were 5.0×10^3 m³/year and 16.6×10^3 m³/year, respectively, indicating that the outflow rate is greater than the inflow. Between wells R17 and L34, the Echi River is located, and the river water recharges the groundwater in this district (contour in Fig. 4a). Thus, the increasing outflow rate in S4 could be considered as the recharging of river water.

In C–C', the groundwater budget in six segments is shown in Fig. 5b. The vertical outflow rates from UCI to CI at S1, S2, and S3 were 123.2×10^3 m³/year, 55.0×10^3 m³/year, and 36.9×10^3 m³/year, respectively, and the inflow rate at S4 in CI was 19.6×10^3 m³/year. It indicates that the groundwater infiltrates deeper aquifers than CI near the foot of mountains. At S4, S5, and S6, the vertical outflow rate from UCI to CI was 3.5×10^3 m³/year, 5.7×10^3 m³/year, and 2.7×10^3 m³/year, respectively. These values are an order of magnitude lower than the cross-sectional flow rate at wells L12, L19, and L28 in UCI. This may indicate that the horizontal flow is dominant in the unconfined aquifer in C–C'. The amounts of the vertical outflow to ATI at S4 and S5 might be considered as the pumping rates, but the rate was lower than that of B–B'.

Discussion

Vertical outflow rate from the unconfined aquifer to the confined aquifer

The outflow rates from the unconfined aquifer (UCI) to the confined aquifer of B–B' (CII) and C–C' (CI) showed different values. The hydraulic potential lines in B–B' and C–C' indicated a different shape (Fig. 4c). In general, the groundwater perpendicularly flows through the hydraulic potential lines. Thus, it can be considered that the unconfined groundwater in B–B' flows downward and that of C–C' flows in horizontal directions. To further understand the difference of the outflow rates, the fluid velocity was calculated using Eq. (8) at well R17 and L19. These are observation wells drilled for measuring the groundwater level of unconfined and confined aquifers separately. According to Yang et al. (2011), the groundwater level of UCI at R17 was 145 m and the groundwater head of CII was 139 m. The distance between UCI and CII screens was 55 m. Assuming that the hydraulic conductivity and porosity are 7.4×10^{-5} m/s and 0.1, respectively, the fluid velocity (v_r) at R17 was calculated to be 8.1×10^{-5} m/s. Similarly, the groundwater level of UCI at L19 was 164 m and the groundwater head of CI was 163.3 m with 35 m of the screen distance. From the same values of the hydraulic conductivity and porosity, the fluid velocity (v_r) at L19 was calculated to be 1.5×10^{-5} m/s, indicating the fluid velocity of CI is lower than that of CII.

In this study, the results of outflow rates from the unconfined aquifer (UCI) to the confined aquifer of C–C' (CI) showed a one-order of magnitude lower value than that of B–B' (CII). The fluid velocities at R17 and L19 were calculated using the same values of the hydraulic conductivity and porosity, but the hydraulic gradient was significantly different (i.e., 0.11 in B–B' and 0.02 in C–C'). Therefore, it may conclude that the difference of the hydraulic gradient causes the difference of the vertical outflow rates from the unconfined aquifer of B–B' and C–C'. The difference of the hydraulic gradient might be derived from the different aquifer structures between B–B' and C–C'. The main aquitards in B–B' and C–C' are ATII and ATI, which is corresponded to Uriuzutoge Member and Hino Clay Member, respectively. The Uriuzutoge Member is a younger formation than Hino Clay Member and contains slightly gravels in it (Table 1), which may allow some groundwater to flow vertically.

Comparison between the flow rate and the groundwater flow

Figure 6 shows the aquifer structure of B–B' and C–C' with the groundwater temperature (Yang et al. 2011), the
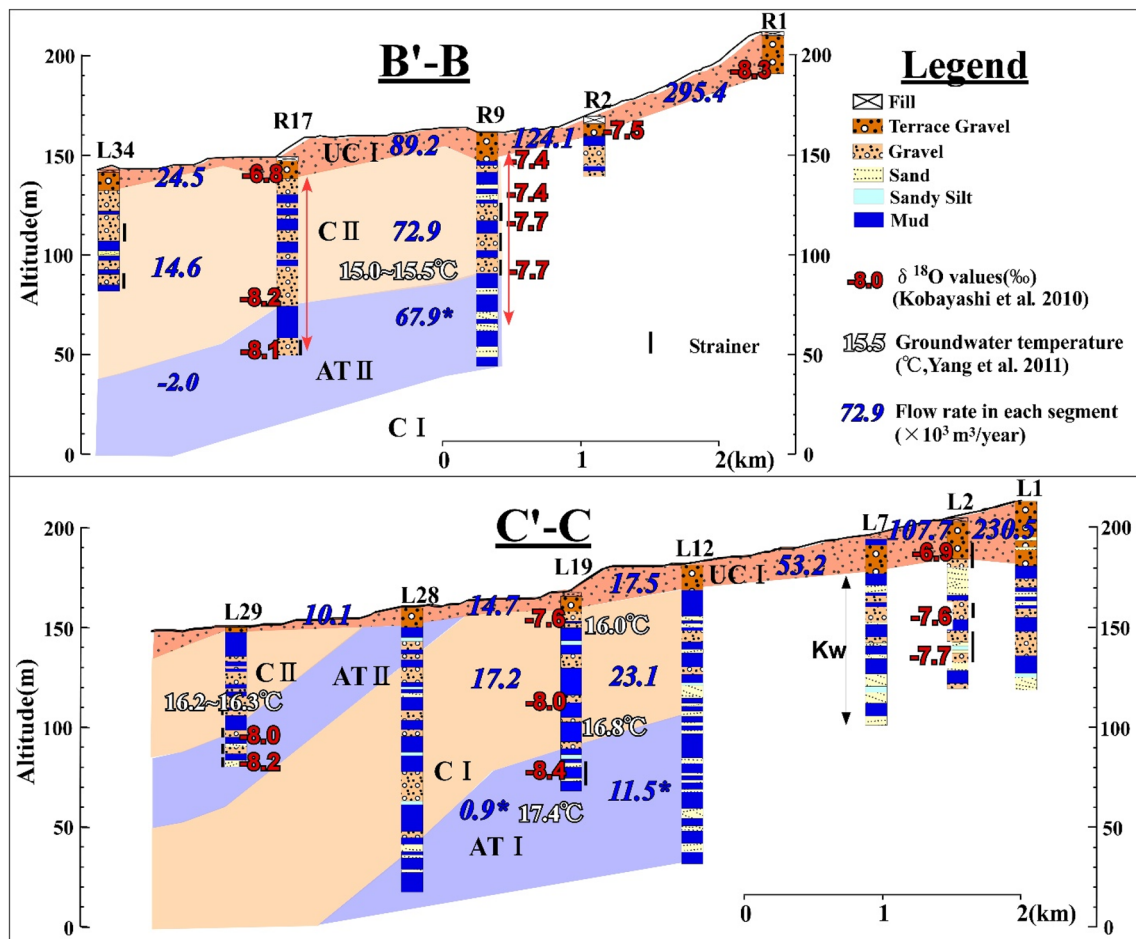
Fig. 6 Aquifer structures of *B–B′* and *C–C′* with the groundwater temperature (Yang et al. 2011; white numbers), the oxygen isotope ratio (δ18O, Kobayashi et al. 2010; red numbers), and the changes in groundwater storage of each segment (this study; blue numbers). UCI is unconfined aquifer; CI and CII are confined aquifers; ATI and ATII are aquitards. Altitude indicates meter above sea level

oxygen isotope ratio (δ18O; Kobayashi et al. 2010), and the changes in groundwater storage of each segment. In *B–B′*, the total flow rate in UCI is 533.2 × 10³ m³/year, of which the outflow to CII is 14%, except for S1 and S2, because they infiltrate deeper aquifers. The groundwater temperature converges from 15.0 to 15.5 °C in the UCI, CII, and ATII (Fig. 6a). The δ18O value shows relatively heavy values of − 6.8 to − 7.7‰ at wells R2, R9, and R17, but it has light values of − 8.1 to − 8.3‰ at wells R1 and R17. Especially, the δ18O value at wells R9 indicates a heavier value than that of R17 in CII (Fig. 6a). The heavier value of δ18O at well R9 suggests that the groundwater flows downward, because the source of the heavier δ18O value is irrigation water and lowland rainfall. In addition, the light values of − 8.1 to − 8.3‰ around 80 to 100 m in altitude are probably derived from water recharged in the mountain and river (Kobayashi et al. 2010). In the result section, it was carefully concluded that the vertical flow rate to ATII is the pumping rate, because ATII is an aquitard, and the

sustained groundwater pumping is taking place near S3. Although the ATII aquitard allows slightly the confined groundwater to infiltrate, it is reasonable that the groundwater pumping affects the groundwater flow based on the result of the heavier δ18O value at well R9. Therefore, it may assume that the groundwater pumping accelerates downward flow (from UCI to CII), and groundwater flowing downward reaches the boundary of the ATII and CII at well R9. It affects the heavier δ18O value of − 7.7‰ in the lower part of the CII, which means that deterioration of water quality, if it occurs, may reach to the confined aquifer.

In *C–C′*, the total flow rate in UCI is 433.7 × 10³ m³/year, of which the outflow to CI is 2.7%, indicating the lower amount than that in *B–B′*. The unconfined groundwater temperature converges from 16.0 to 16.3 °C in CII and upper CI (Fig. 6b). The confined groundwater temperature rises from 16.0 to 17.4 °C with depth (Fig. 6b). The δ18O value has heavy values of − 6.8 to − 7.7‰ in CII and the upper CI

and light values of − 8.0 to − 8.2‰ in ATII and the middle of CI. The lightest value of − 8.4‰ was confirmed in ATI. Especially, the $\delta^{18}O$ value shows the light values of − 8.0‰ in CI and of − 8.4‰ in ATI at well L19 (Fig. 6b). The vertical outflow rates to the ATI aquifer were considered as the pumping rates in the same way as *B–B′*. However, results of the increasing groundwater temperature, the lighter $\delta^{18}O$ value, and an order of magnitude lower outflow rate than those of *B–B′* suggest that the pumping rate is lower than that of *B–B′*. In addition, the upward groundwater flow from ATI to CI at well L19 may happen considering the hydraulic potential line of 165 m around ATI (Fig. 4c). However, separating the groundwater pumping and the upward groundwater flow rate using the groundwater budget this study provided is unavailable, because the hydraulic head data in ATI exist only at well L19. Therefore, the author concludes qualitatively that upward groundwater flow indicating 17.4 °C and − 8.4‰ in ATI has a somewhat role in forming the temperature and the $\delta^{18}O$ value in CI at well L19.

In the study, the flow rates in each segment in *B–B′* and *C–C′* were calculated based on the cross-sectional groundwater flow systems using the groundwater budget. The results well correspond to the previous studies, but this study found that the groundwater pumping and the seepage from the aquitard somewhat affect the groundwater flow in the confined aquifer in *C–C′*. To elucidate the unsolved issue, further analysis such as the measurement of the hydraulic head at the field and three-dimensional numerical modeling is necessary, which will be a future study.

Conclusions

The present study was conducted to quantitatively ascertain the groundwater flow using the groundwater budget by combining hydrogeological parameters (hydraulic gradient, hydraulic conductivity, and recharge rate) and modified aquifer structures (unconfined/confined aquifers and aquitards) at the Echi-gawa alluvial fan, Japan. The groundwater budget was calculated on the right bank (*B–B′*) and left bank (*C–C′*) of the Echi River, where the aquifer structures are significantly different, and the groundwater flow paths are dominant.

The cross-sectional flow rates were calculated at five wells in *B–B′*. The flow rates from well R1 to well L34 in the unconfined aquifer (UCI) were decreased as the groundwater flows from the mountain area to the Echi River. The flow rates in the confined aquifer (CII) indicated relatively lower flow rates than those of the unconfined aquifer. In *C–C′*, the cross-sectional flow rates were calculated at seven wells. The flow rates from well L1 to well L29 in the unconfined aquifer were decreased the same as *B–B′*. The flow rates in

the confined aquifer (CI) showed the same magnitude of the unconfined aquifer at wells L12. L19. and L28.

The groundwater budget was conducted in four and six segments in *B–B′* and *C–C′*, respectively. The vertical outflow rates from the unconfined aquifer to the confined aquifer near the foot of mountains indicated that 5–20-holds amount of the groundwater infiltrates to more deeper aquifers than the confined aquifer. From the comparison of the $\delta^{18}O$ value, the groundwater pumping may accelerate downward flow (from UCI to CII) at well R9 in *B–B′*. In *C–C′*, the vertical outflow rate from UCI to CI at S4, S5, and S6 showed an order of magnitude lower than the cross-sectional flow rate at wells L12, L19, and L28 in UCI. This may indicate that the horizontal flow is dominant in the unconfined aquifer. The difference of the vertical outflow rates from the unconfined aquifers of *B–B′* and *C–C′* is derived from the different aquifer structures between *B–B′* and *C–C′*.

Results of the groundwater budget in this study are well corresponded to the previous studies. Although separating the groundwater pumping and the upward groundwater flow rate using the groundwater budget this study provided is unavailable due to lack of the hydraulic head data in ATI, the method used for this study is adequate to reproduce groundwater flow systems, which may support evaluation of the groundwater flow quantitatively on the other alluvial fan areas.

Declarations

References

Alattar MH, Troy TJ, Russo TA, Boyce SE (2020) Modeling the surface water and groundwater budgets of the US using MOD-FLOW-OWHM. Adv Water Resour 143:103682. https://doi.org/10.1016/j.advwatres.2020.103682

Alley WM, Leake SA (2004) The journey from safe yield to sustainability. Groundwater 42(1):12–16

Barackman M, Brusseau ML (2002) Groundwater sampling. In: Artiola JF, Pepper IL, Brusseau ML (eds) Environmental monitoring and characterization. Academic Press, Burlington, pp 121–139

Cervi F, Tazioli A (2021) Quantifying streambed dispersion in an alluvial fan facing the northern Italian Apennines: implications for groundwater management of vulnerable aquifers. Hydrology 8(3):118. https://doi.org/10.3390/hydrology8030118

Demiroglu M (2019) Groundwater budget rationale, time, and regional flow: a case study in Istanbul, Turkey. Environ Earth Sci 78:682. https://doi.org/10.1007/s12665-019-8713-2

Earle S (2019) Physical geology, 2nd edn. BCcampus, Victoria. Retrieved from https://opentextbc.ca/physicalgeology2ed/. Accessed 28 Dec 2021

England LA, Freeze RA (1988) Finite-element simulation of long-term transient regional groundwater flow. Groundwater 26:298–308

Genereux DP, Jordan MT, Carbonell D (2005) A paired-watershed budget study to quantify interbasin groundwater flow in a lowland rain forest, Costa Rica. Water Resour Res 41:1–17

Gu XM, Shao JL, Cui YL, Hao QC (2017) Calibration of two-dimensional variably saturated numerical model for groundwater flow in arid inland basin, China. Curr Sci 113:403–412

Hamada T, Yamada M, Ao L, Horiuchi K, Yang H, Kobayashi M, Nonomura O (2008) Groundwater flow system in alluvial fan of Echi-gawa traced by groundwater potential, water quality and isotopic compositions. In: Hydro-environments of Alluvial Fans in Japan, Research group on hydro-environment around alluvial fans, Toyama, pp 211–222 (**in Japanese**)

Harayama S, Miyamura M, Yoshida F, Miura K, Kurimoto C (1989) Geology of the Gozaishoyama district, with geological sheet map at 1:50,000. Geol Surv Jpn 30:1–145 (**in Japanese**)

He B, Takase K, Wang Y (2008) Numerical simulation of groundwater flow for a coastal plain in Japan: data collection and model calibration. Environ Geol 55:1745–1753

Hijii T, Kayaki T, Watanabe O, Oishi A, Hamada T, Kobayashi M (2008) Water budget of the Echi-gawa alluvial fan-simulation results-. In: Hydro-environments of Alluvial Fans in Japan, Research group on hydro-environment around alluvial fans, Toyama, pp 191–210

Horino H, Watanabe S, Maruyama T (1989) Study of an actual demonstrations on the role of groundwater in agriculture water utilization. Pap Ser Agric Eng 144:9–16 (**in Japanese**)

Ibrakhimov M, Awan UK, George B, Liaqat UW (2018) Understanding surface water–groundwater interactions for managing large irrigation schemes in the multi-country Fergana valley, Central Asia. Agric Water Manag 201:99–106

Ikeda H, Ohashi T, Uemura Y, Yoshikoshi A (1979) Geomorphology of the Ohmi Basin. In: Land and Life in Shiga-Seperate Volume for Geomorphology and Geology and Geologic Map of Shiga Prefecture 1:100,000 in Scale. Shiga Prefecture Nature Conservation Foundation, Japan, pp 1–112 (**in Japanese**)

Japanese Geotechnical Society (2005) Ground survey-Basic and Guidance. Maruzen Publishing, Tokyo (**in Japanese**)

Kobayashi M, Hijii T, Yang H, Hamada T (2008) Relations between groundwater and river water in the Echi-gawa alluvial fan. In: Hydro-environments of Alluvial Fans in Japan, Research group on hydro-environment around alluvial fans, Toyama, pp 223–234

Kobayashi M, Yamada M, Yang H, Hijii T (2010) Study of the groundwater flow system in the Echi-gawa alluvial fan, Shiga Prefecture, Japan. In: Taniguchi M and Holman IP (eds) Groundwater response to changing climate. Taylor & Francis Group, London, UK, pp 179–195

Lu CY, Hu JC, Chan YC, Su YF, Chang CH (2020) The relationship between surface displacement and groundwater level change and its hydrogeological implications in an alluvial fan: case study of the Choshui River, Taiwan. Remote Sens 12(20):3315. https://doi.org/10.3390/rs12203315

Nishimura S (1979) Gravity survey in Shiga Prefecture. In: Land and Life in Shiga-Seperate Volume for Geomorphology and Geology and Geologic Map of Shiga Prefecture 1:100,000 in Scale. Shiga Prefecture Nature Conservation Foundation, Japan, pp 469–478 (**in Japanese**)

Oishi A, Kobayashi M, Hamada T, Okuda E, Miyazaki S, Hu S (2008) Hydrogeology on Echi-gawa alluvial fan, Shiga Prefecture, Central Japan. In: Hydro-environments of Alluvial Fans in Japan,

Research group on hydro-environment around alluvial fans, Toyama, pp 191–210

Sakata Y, Baran G, Suzuki T, Chikita A (2016) Estimate of river seepage by conditioning downward groundwater flow in the Toyohira River alluvial fan, Japan. Hydrol Sci J 61:1280–1290. https://doi.org/10.1080/02626667.2015.1125481

Sakura Y (1984) Groundwater investigation using temperature. J Groundw Hydrol 26:193–197

Shimada J, Ito S, Arakawa Y, Tada K, Mori K, Nakano K, Kagabu M, Matsunaga M (2015) Nitrate budget in the shallow unconfined groundwater of double cropped paddy area considering chemical fertilizer input—results of 3D groundwater flow simulation with observed water chemistry data. J Groundw Hydrol 57(4):467–482. https://doi.org/10.5917/jagh.57.467 (**in Japanese**)

Takase K, Fujihara Y (2019) Evaluation of the effects of irrigation water on groundwater budget by a hydrologic model. Paddy Water Environ 17:439–446

Thornthwaite CW (1948) An approach toward a rational classification of climate. Geogr Rev 38:55–94

Tóth J, Hayashi M (2010) The theory of basinal gravity flow groundwater and its impacts on hydrology in Japan. J Groundw Hydrol 52:335–354

Tóth J, Millar RF (1983) Possible effects of erosional changes of the topographic relief on pore pressure at depth. Water Resour Res 19:1585–1597

Viaroli S, Mastrorillo L, Lotti F, Paolucci V, Mazza R (2018) The groundwater budget: a tool for preliminary estimation of the hydraulic connection between neighboring aquifers. J Hydrol 556:72–86

Xiao Y, Hao Q, Zhang Y, Zhu Y, Yin S, Qin L, Li X (2022) Investigating sources, driving forces and potential health risks of nitrate and fluoride in groundwater of a typical alluvial fan plain. Sci Total Environ. https://doi.org/10.1016/j.scitotenv.2021.149909

Yamamoto S (1983) Method of the groundwater survey. Kokon Shoin, Tokyo (**in Japanese**)

Yamanaka M, Sakamoto K (2016) Hydrogeochemical controls of groundwater in the Ohmama Alluvial Fan in Gunma Prefecture. J Groundw Hydrol 58(2):165–181 (**in Japanese**)

Yang H, Mitamura M (2012) Evaluation of the aquifer structure and the groundwater flow in the Echigawa alluvial fan area, Shiga Prefecture, Japan. J Geosci Osaka City Univ 55:1–10

Yang H, Kobayashi M, Mitamura M (2011) Groundwater flow and formation of groundwater temperature in the Echi-gawa Alluvial Fan, Shiga Prefecture, Japan. J Groundw Hydrol 53(2):165–177. https://doi.org/10.5917/jagh.53.165 (**in Japanese**)

Yin S, Xiao Y, Gu X et al (2019) Geostatistical analysis of hydrochemical variations and nitrate pollution causes of groundwater in an alluvial fan plain. Acta Geophys 67:1191–1203. https://doi.org/10.1007/s11600-019-00302-5

Yokoyama T, Matsuoka C, Tamura M, Amemori K (1979) On the Plio-Pleistocene Kobiwako Group, land of life in Shiga, pp 309–389 (**in Japanese**)

Zhou Y (2009) A critical review of groundwater budget myth, safe yield and sustainability. J Hydrol 370:207–213